Astron. Astrophys. 355, 327–332 (2000)

ASTRONOMY AND ASTROPHYSICS

# SiO in diffuse, translucent and 'spiral-arm' clouds

**R. Lucas**[1] **and H.S. Liszt**[2]

[1] Institut de Radioastronomie Millimétrique, 300 Rue de la Piscine, 38406 Saint Martin d'Hères, France
[2] National Radio Astronomy Observatory, 520 Edgemont Road, Charlottesville, VA 22903-2475, USA

Received 28 September 1999 / Accepted 5 January 2000

**Abstract.** Using the Plateau de Bure interferometer, we searched for thermal SiO J=1-2 absorption at 86 GHz from the diffuse and translucent clouds which lie toward our sample of extragalactic continuum sources. SiO is present at a level N(SiO)/N($HCO^+$) $\approx$ $0.01 - 0.1$, or N(SiO)/N($H_2$) $\approx$ $2 \times 10^{-11} - 2 \times 10^{-10}$. N(SiO) declines with increasing N($HCO^+$) and with increasing thermal pressure measured in the J=1-0 lines of CO. SiO is grossly underabundant, even compared to the known gas-phase depletion of Si in diffuse clouds.

To pursue the subject further, we mapped the $H^{13}CO^+$ J=1-0 and SiO J=2-1 lines toward the core of W49A: SiO and many other molecular absorption lines have been studied in 'spiral-arm' clouds seen along the galactic plane at v = 40 and 60 km s$^{-1}$ using single dishes. $H^{13}CO^+$ absorbs quite strongly at these velocities, with column densities at least 3-4 times larger than in any of the clouds we have studied toward extragalactic sources. But SiO absorption is absent at 40 km s$^{-1}$ and perhaps at 60 km s$^{-1}$ as well since the latter is overlaid by a series of dimethyl ether lines originating in the dense core of the W49A molecular gas: the dimethyl ether was not recognized as such in singledish absorption profiles. Our upper limit for SiO in the 'spiral-arm' cloud at 40 km s$^{-1}$ is consistent with the trends seen in the more diffuse gas at higher galactic latitudes toward the extragalactic sources.

**Key words:** ISM: abundances – ISM: clouds – ISM: molecules – ISM: structure – radio lines: ISM

## 1. Introduction

Interstellar silicon has an exceptionally quirky chemistry in galactic molecular gas, with an abundance ranging from N(SiO)/N($H_2$) $< 5 \times 10^{-12}$ in dark clouds (Ziurys et al. 1989) to N(SiO)/N($H_2$) $\approx$ $1 - 10 \times 10^{-8}$ in shocked regions and molecular outflows (Lefloch et al. 1998; Liu et al. 1998). Intermediate values N(SiO)/N($H_2$) $\approx$ $10^{-10}$ are seen in six of Turner's small high-latitude translucent clouds ($\approx$ $10^{-11}$ in the other 20, Turner 1998), and N(SiO)/N($H_2$) $\approx$ $10^{-10}$ (Greaves et al. 1996) or $\approx$ $10^{-9}$ (Greaves & Nyman 1996) from singledish absorption spectra of clouds which coincidentally occur in the galactic plane toward low latitude molecular cloud/HII region complexes like Sgr B2, W49A, and W51. It is thought that silicon is largely tied up in interstellar grains in dark dense clouds, with depletions above 0.9999, and released only with passage through the gas of a shock or some other, similarly disruptive event (Schilke et al. 1997).

Here we report the results of two mm-wave interferometer-based experiments pursuing the somewhat elusive goal of studying thermal SiO in absorption from diffuse gas. Using the Plateau de Bure Interferometer, we looked first toward a few extragalactic continuum sources whose spectra we have studied extensively in such common species as CO, $HCO^+$ OH, HCN, HNC, $C_2H$ ... $etc$ (Lucas & Liszt 1998; Liszt & Lucas 1998; Liszt & Lucas 1996; Lucas & Liszt 1996): along such lines of sight we find N(SiO)/N($HCO^+$) $\approx 0.01 - 0.1$ or N(SiO)/N($H_2$) $\approx 2 \times 10^{-11} - 2 \times 10^{-10}$.

We then synthesized $H^{13}CO^+$ and SiO emission and absorption toward the core of the W49A molecular cloud/HII-region complex (Mufson & Liszt 1977) which lies near the sub-central point along the line of sight at $l = 43.2°$, $b = 0°$. In this direction, two heavily-studied 'spiral-arm' clouds appear in absorption at 40 and 60 km s$^{-1}$ in singledish profiles. In our data, $H^{13}CO^+$ is easily seen in both clouds, and in a broader feature near the terminal velocity corresponding to distributed gas in the galactic disk. $^{13}CO$ emission is easily found. But we did not see any sign of SiO absorption toward W49A at 40 km s$^{-1}$, and the other line – whose SiO absorption was discounted by Greaves et al. (1996) owing to a slightly aberrant velocity– is either contaminated by a series of dimethyl ether lines produced in the dense core of the W49A molecular cloud or is simply their blue absorption wing.

Sect. 2 describes the observational material used here, basically the point-source absorption profiles of SiO and $HCO^+$ toward extragalactic sources and the new maps of SiO and $H^{13}CO^+$ toward the core of W49A. Sect. 3 is a discussion of this material; Sect. 4 discusses the relationship between 'spiral-arm' clouds and those we have studied at higher latitudes and the relevance of trends in the interstellar Si/SiO chemistry.

*Send offprint requests to*: R. Lucas
*Correspondence to*: rlucas@iram.fr

**Table 1.** Background Sources and Line/Continuum Rms

| Source | Alias | l ° | b ° | $\sigma_{l/c}$ SiO | $\sigma_{l/c}$ SiS |
|---|---|---|---|---|---|
| B0355+508 | NRAO 150 | 150.38 | −1.60 | 0.0120 | |
| B0415+379 | 3C 111 | 161.68 | −8.82 | 0.0073 | 0.0645 |
| B0528+134 | | 191.37 | −11.01 | 0.0150 | 0.0256 |
| B1730−130 | NRAO 530 | 12.03 | 10.81 | 0.0034 | 0.0110 |
| B2251+158 | 3C 454.3 | 86.11 | −38.18 | 0.0089 | 0.0170 |

**Table 2.** SiO and $HCO^+$ line profile integrals

| Source | Interval km s$^{-1}$ | $\int \tau(\mathrm{SiO})dv$ km s$^{-1}$ | $\int \tau(\mathrm{HCO^+})dv$ km s$^{-1}$ |
|---|---|---|---|
| B0355+508 | (-19.3,-16.1) | -0.024(0.012) | 1.00 |
| | (-15.4,-12.0) | 0.031(0.012) | 1.13 |
| | (-11.6,-9.7) | -0.010(0.010) | 1.07 |
| | (-9.5,-7.2) | 0.021(0.010) | 0.95 |
| | (-5.9,-1.5) | 0.050(0.014) | 0.94 |
| B0415+379 | (-3.9,-2.3) | 0.0155(0.0029) | 4.06 |
| | (-2.3,-0.4) | 0.0205(0.0031) | 7.26 |
| B0528+134 | (-0.5,5.3) | 0.053(0.030) | 0.22 |
| | (7.0,11.0) | -0.020(0.026) | 1.86 |
| B1730−130 | (3.4,9.3) | 0.0376(0.0048) | 1.11 |
| B2251+158 | (-11.9,-8.4) | 0.0064(0.0166) | 0.28 |

## 2. Observations

### *2.1. SiO and SiS toward compact extragalactic continuum sources*

During the period 1994 - 1996 we took SiO and SiS J=1-2 absorption spectra toward the sources listed in Table 1, with the the Plateau de Bure Interferometer, using the same techniques described in earlier members of this series of papers (*e.g.* Lucas & Liszt 1998; Liszt & Lucas 1998). The channel separation and velocity resolution of the SiO data are 0.270 and 0.484 km s$^{-1}$, respectively, and 0.258 and 0.462 for SiS. Using standard molecular constants, and in the limit of no collisional excitation ($T_{\rm exc}$ assumed constant and equal to 2.73 K), the column densities of these species are related to their integrated optical depth in the J=1-2 transition by N(X) = $\mathrm{A}_X \int \tau_{1-2}(X)dv$ where $\mathrm{A}_{SiO} = 3.39 \times 10^{12}$ cm$^{-2}$ and $\mathrm{A}_{SiS} = 1.07 \times 10^{13}$ cm$^{-2}$. Results are in Table 2. Use of the weak-excitation limit is justified for diffuse clouds by the weakness of their $HCO^+$ emission as discussed by Lucas & Liszt (1996). For the 'spiral-arm' clouds, which have been claimed to be of relatively low density, but which we infer to be of higher column and higher number density, the true column densities will be higher than are given by this estimate. This situation is discussed briefly in Sect. 3.2.

### *2.2. $H^{13}CO^+$ and SiO toward W49A*

In 1998 May to July we observed the core of the W49A molecular cloud/HII-region complex in both the J=1-0 transition of $H^{13}CO^+$ and the SiO J=2-1 transition (each seen in both emission and absorption). As will be shown below, dimethyl ether lines, appearing at about +60 km s$^{-1}$ with respect to the zero of velocity for SiO, are detected in emission, and perhaps in absorption, as well. This complicates interpretation of parts of the SiO spectrum over which we had hoped to see absorption from the 'spiral-arm' clouds discussed by Greaves et al. (1996).

Configurations C and D were used, mostly with 4 antennas. The phase calibrator was B1827+062 (0.5 Jy at 86.9 GHz). Amplitude and phase passbands were calibrated using 3C273. The channel separation was 0.54 km s$^{-1}$ and the data were smoothed to 0.8 km s$^{-1}$ resolution. The synthesized beam is $4.46'' \times 3.57''$ in PA 4°, so that 1 Jy/beam is 10.2 K. The maps were CLEANed in the usual, standard way.

The W49A source itself is extremely complicated, and the combination of emission and absorption from the dense cloud core, coupled with an extended continuum structure, foreground absorption, and beam sidelobes of both the emission and absorption, quickly convinced us not to attempt an explanation of the source structure on the basis of our limited observations.

## 3. The quest for SiO J=1-2 absorption

### *3.1. Toward extragalactic sources*

Profiles of the SiO data are compared with those of $HCO^+$ (Lucas & Liszt 1996 and our work in progress) in Fig. 1 for four sources. The clearest detection is toward B1730−130, which has modest $HCO^+$ absorption compared to either B0355+508 or B0415+379. The line of sight toward B1730−130 is interesting in that it is one of the few where there is a noticeable difference in the morphologies of OH and $HCO^+$ (our forthcoming work): the weaker feature in the red wing of the $HCO^+$ profile is missing in OH. In general, OH is expected to be more widely distributed in space and velocity because it can easily be made in both quiescent and shocked gas, and when local dissipation of turbulent energy is invoked to account for species like $HCO^+$ which are more efficiently synthesized in endothermic reactions (Flower & Pineau Des Forêts (1998); Joulain et al. 1998). The presence of SiO across the entire range of $HCO^+$ absorption suggests that the two clear kinematic components seen in $HCO^+$ are physically associated. The SiO/$HCO^+$ ratio is much larger in the weaker red wing but the SiO profile does not lend itself to an easy decomposition.

A plot of N(SiO) and N($HCO^+$) is shown in Fig. 2. The column densities were formed by taking profile integrals over the ranges occupied by the most obvious kinematic components present in $HCO^+$, as listed in Table 2. Toward B0415+379, the $HCO^+$ column density was derived by gaussian fitting since the optical depth is so high. Toward B1730−130 and B2251+158 the entire profiles were used. The data for B0528+134 are not plotted since the limits on N(SiO) are so poor.

In the plots, datapoints with less than a $2\sigma$ detection are shown as $2\sigma$ upper limits. Fig. 2 compares profile integrals and glosses over the possible velocity differences; if SiO is present toward B0355+508, it may exhibit a slight preference for the interstices of the $HCO^+$ absorption. In the plots, the putative SiO feature at -1 km s$^{-1}$toward B0355+508 is likewise ignored.

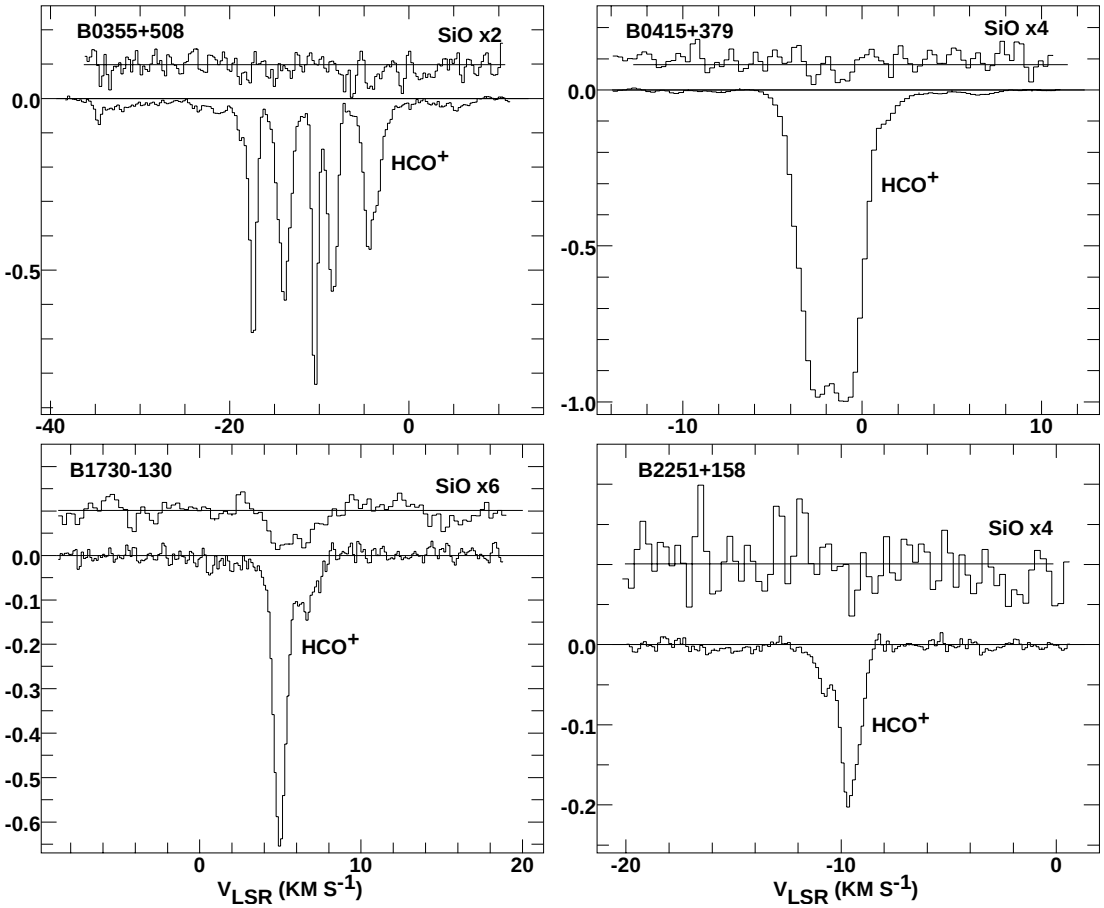


**Fig. 1.** SiO J=1-2 and $HCO^+$ J=0-1 absorption spectra as line/continuum ratios. The SiO spectra are shown above the $HCO^+$ spectra and have been scaled as indicated

The highest column densities of SiO are in the gas at v $\gtrsim -10$ km s$^{-1}$ toward B0355+508 and toward B1730−130 (outlined). If there is any systematic variation, N(SiO)/N($HCO^+$) declines markedly with N($HCO^+$). This ratio is in the range $0.12 \pm 0.05$ at N($HCO^+$) = $1 \times 10^{12}$ cm$^{-2}$, and 0.01 for either of the lines toward B0415+379 (which have the highest N($HCO^+$)). If N($HCO^+$)/N($H_2$) $\approx 2 \times 10^{-9}$ it follows that N(SiO)/N($H_2$) declines from about $2-3\times10^{-10}$ to $2\times10^{-11}$.

Most of the clouds observed in SiO have N($HCO^+$) $\approx 10^{12}$ cm$^{-2}$. The SiO data can be made to appear less random if they are plotted against the excitation temperature of the $^{12}$CO J=1-0 line, which is proportional to n($H_2$)$T_k$ under a wide range of conditions in diffuse clouds (Liszt & Lucas 1998). Apparently, the SiO abundance wanes at higher thermal pressure.

### *3.2. Toward W49A*

Because of the haphazard and rather marginal nature of the appearance of the SiO seen toward the extragalactic objects, and reasoning that a long line of sight through the galactic disk would present interesting possibilities, we resorted to study of the 'spiral-arm' clouds whose singledish absorption spectra against Sgr B2, W51, and W49A have been used to deduce molecular abundances in a population which is claimed to overlap the regimes described as 'translucent' and 'dark' (Greaves & Nyman 1996). However the results here also were not as expected, necessitating a somewhat detailed explanation of a variety of spectra taken toward W49A. As a first step, we establish the identity of the 'spiral-arm' clouds in the context of the present observations and present SiO spectra at the continuum peak and averaged over the area of a typical 15″ singledish beam.

In the bottom panel of Fig. 3 we show the spectrum of $^{13}$CO J=1−0 emission seen recently at the NRAO 12-m antenna toward the continuum peak of W49A, and (shaded) the H$^{13}$CO$^+$ emission/absorption seen toward the peak at the Plateau de Bure: the continuum flux density at the continuum peak is 1.84 Jy/beam. H$^{13}$CO$^+$ is seen in two discrete features at 39.1 and 60.1 km s$^{-1}$ arising in the so-called 'spiral-arm' clouds with N(H$^{13}$CO$^+$) $> 3.1 \times 10^{11}$ cm$^{-2}$ and $> 3.7 \times 10^{11}$ cm$^{-2}$ respectively; the lower limits arise because the 'spiral-arm' clouds are likely to be denser and darker than the diffuse clouds seen at higher latitudes, so that collisional excitation is not entirely negligible. There is also a broader wing of H$^{13}$CO$^+$ absorption between 40 and 65 km s$^{-1}$ representing distributed gas in the plane which is 'velocity-crowded' into a ridge near the terminal velocity due to geometrical effects. Only a portion of this high-velocity absorption wing is seen in $^{13}$CO emission and

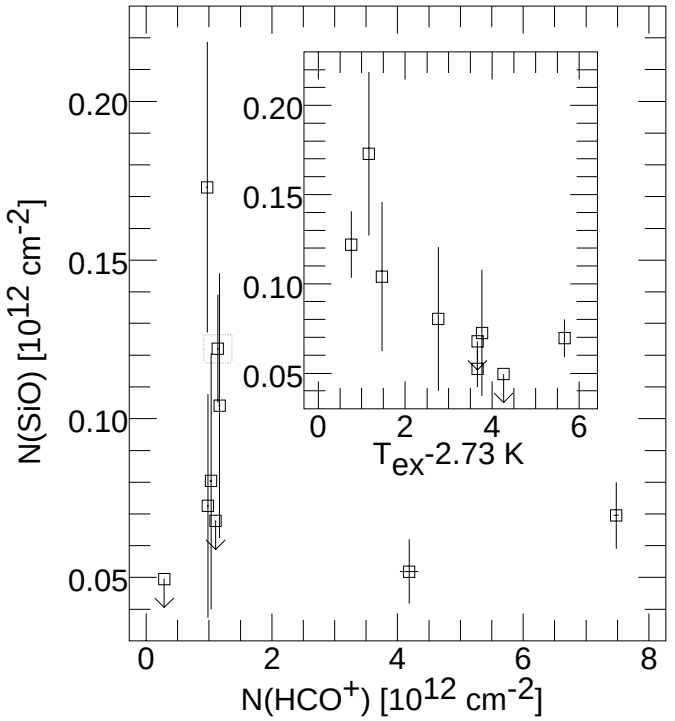


**Fig. 2.** SiO and $HCO^+$ column densities compared. The line of sight toward B1730-130 is outlined. The highest SiO column density is in the material at $v \gtrsim -10$ km s$^{-1}$ toward B0355+508 (see Fig. 1). Inset: The same SiO column densities reordered to appear $vs$ the CO J=1-0 excitation temperature derived by Liszt & Lucas (1998). In diffuse clouds, the CO excitation temperature is proportional to the ambient partial pressure of $H_2$

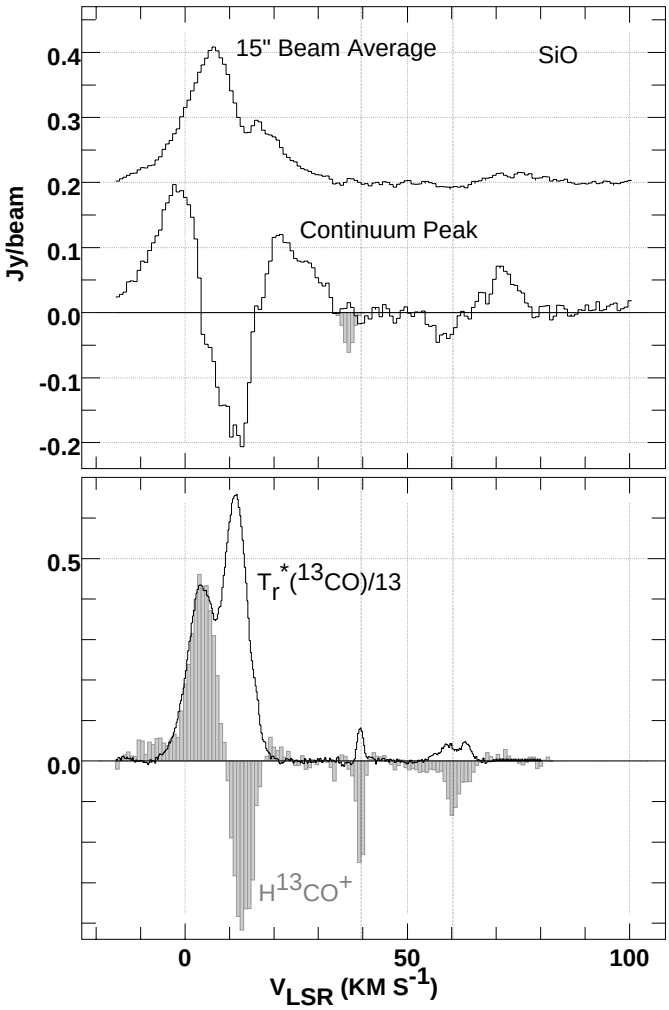


**Fig. 3.** SiO, $^{13}$CO, and $H^{13}CO^+$ spectra toward and around W49A. Top: SiO toward the continuum peak ($S_\nu$ = 1.84 Jy/beam) and averaged with a 15″ gaussian taper ($\langle S_\nu \rangle$ = 0.24 Jy/beam). Note the emission feature at 70 km s$^{-1}$ from a series of dimethyl ether lines arising in the hot, dense, chemically-complex core of the W49A molecular cloud. The narrow grayed absorption feature toward the continuum peak is a representation (not data) of the 'spiral-arm' clouds SiO absorption feature described by Greaves et al. (1996). Bottom: a scaled spectrum of $^{13}$CO J=1−0 emission from the 1′ beam of the 12-m telescope (in units of Kelvins) and the Plateau de Bure interferometer profile of $H^{13}CO^+$ (seen simultaneously in both emission and absorption) at the continuum peak (in Jy/beam). Both species have narrower lines than does the SiO. The $H^{13}CO^+$ absorption features at 40 and 60 km s$^{-1}$ differ markedly from those appearing at top

neither the $HCO^+$ nor the $^{13}$CO extends as high in velocity as the features in the SiO spectrum at the top of Fig. 3.

In Fig. 3 in the upper panel we show SiO J=2−1 profiles toward the continuum peak (1.84 Jy/beam) and formed by averaging profiles with a 15″ gaussian taper centered on the continuum peak (to represent singledish data taken at Nobeyama by Greaves et al. (1996)). The scaling of this averaged spectrum is somewhat arbitrary. As shown, so that it can easily be compared with the 4″ resolution spectrum toward the peak, it has been scaled by a factor of 1/15 (approximately the ratio of areas in 4″ and 15″ beams). Although it is not obvious from the Figure, the optical depth in the spectral feature just below 60 km s$^{-1}$ is nearly the same in both profiles, and the averaged profile samples a flux which is almost 4 Jy. In agreement with the singledish profiles, the "self-absorption" from gas within W49A disappears when an average is taken over a region (only slightly) larger than 4″.

Now we are in a position to discuss the appearance of the 'spiral-arm' clouds in SiO spectra. In general, the "SiO" profiles are complex but lack good analogues of the $H^{13}CO^+$ absorption and $^{13}$CO emission features which define the 'spiral-arm' clouds. Shown overlaid on the SiO profile at the continuum peak in Fig. 3 (in gray at top) is a realization of a line which fits the particulars of the feature used by Greaves et al. (1996) to derive the column density N(SiO) $= 3 \times 10^{11}$ cm$^{-2}$; it has an integrated optical depth of 0.08 km s$^{-1}$ and fits within the 35−38 km s$^{-1}$ velocity range they noted. Clearly, such a line is absent from our spectrum. Integrating over the region of the spectrum where $H^{13}CO^+$ absorption occurs, around 39 km s$^{-1}$, we have a nominal $2\sigma$ upper limit (ignoring collisional excitation) of $1.3 \times 10^{11}$ cm$^{-2}$ on N(SiO), or N(SiO)/N($H^{13}CO^+$) $< 0.42$: the corresponding ratio for either kinematic component toward B0415+379 is 0.58. So it seems that N(SiO)/N($HCO^+$) $< 0.01$ and N(SiO)/N($H_2$) $< 2 \times 10^{-11}$ toward either the 40

km s$^{-1}$ 'spiral-arm' gas or 3C111. This is somewhat above the relative abundances believed to obtain in dark clouds (Ziurys et al. 1989) but is a factor 30 or more below the values cited for the 'spiral-arm' clouds toward Sgr B2 in Table 6 of Greaves & Nyman (1996).

The strong emission feature at about $+70$ km s$^{-1}$ in the "SiO" spectrum (noticeably higher in velocity than can be seen in $^{13}$CO emission) is actually due to previously-catalogued dimethyl ether lines offset in rest frequency from SiO by the frequency equivalent of +60 km s$^{-1}$: this emission clearly arises in the dense core of the W49A molecular cloud, following that of SiO and H$^{13}$CO$^+$, and is not some unexpected high-density SiO clump in the foreground 'spiral-arm' clouds.

Perhaps because of this emission, the perceived absorption feature just to the blue appears somewhat below 60 km s$^{-1}$, markedly differing from the narrow H$^{13}$CO$^+$ line. Because the corresponding singledish absorption feature seen by Greaves et al. (1996) also appeared at a somewhat too-low velocity, they attributed it to some unknown influence, while noting that the CS and HCN seen in singledish absorption actually share its slightly aberrant behaviour. The dimethyl ether lines do not appear in the published singledish profiles of Greaves et al. (1996) and were probably removed as part of the baseline subtraction of standing waves (which must have been strong) and other seeming artifacts. But, given that there is more flux in the dimethyl ether emission than in the nearby absorption, it should have been easily noticeable.

A different explanation for the aberrant kinematics of the higher-velocity 'SiO' absorption might be that SiO prefers more diffuse gas and therefore appears in the weak broad absorption wing created by velocity crowding, rather than in any of the 'spiral-arm' clouds. Even so, we conclude that, although 'spiral-arm' clouds are real, they are not manifested in SiO toward W49A: the SiO column densities previously derived are unreliable.

### *3.3. W49*

As for W49 itself, most of the flux in the blue wing of the W49A core profile is recovered by the interferometer but the forefront cloud at 11 km s$^{-1}$ appears only in absorption to the interferometer (toward the continuum). SiO emission from the W49A core (Fig. 3 at top) is noticeably broader than that of $^{13}$CO or H$^{13}$CO$^+$, again emphasizing the role of energetic events in regions of high SiO abundance. The SiO emission/absorption profile toward W49A is narrower in velocity but identical in shape to that recently shown for SgrB2(M) by Liu et al. (1998).

### *3.4. SiS*

The SiS measurements are of relatively low quality and do not reach sensitivity levels such that N(SiS) $<$ N(SiO). The most credible limit is toward B1730$-$130, where a $2\sigma$ upper limit on the SiS/SiO ratio is N(SiS)/N(SiO) $< 1.9$; toward 0415 we have N(SiS)/N(SiO) $< 16$ toward either kinematic component.

## 4. Discussion

### *4.1. 'Spiral-arm clouds' in the context of our absorption measurements toward extragalactic continuum sources*

Physical conditions in the 'spiral-arm' clouds are supposed to overlap those we infer for the diffuse and translucent gas occulting extragalactic continuum sources (Liszt & Lucas 1998), which we have studied extensively in a wide variety of molecular and atomic species. Yet, the abundances inferred for the 'spiral-arm' clouds are remarkably different in some important ways. The relative abundance N(CS)/N($H_2$) is shown in Fig. 5 of Greaves & Nyman (1996) as $10^{-7}$ for N($H_2$) $\approx 1\times10^{21}$ cm$^{-2}$, while we find N(CS)/N(HCO$^+$) $\approx$ 1 and N(HCO$^+$)/N($H_2$) $\approx 2\times10^{-9}$ (Liszt & Lucas 1996). The previously-derived abundance of SiO in these 'spiral-arm' clouds, N(SiO)/N($H_2$) $\approx 10^{-9}$ at low N($H_2$) (in that Fig. 5) is much higher than those we infer toward the extragalactic objects and is very large compared to that in dark clouds where Ziurys et al. (1989) find N(SiO)/N(HCN) = 0.0002 $-$ 0.004 or N(SiO)/N($H_2$) $< 5\times10^{-12}$. HCO$^+$, HCN, and HNC are all found to be much more abundant in 'spiral-arm' clouds than in our diffuse/translucent gas (Table 6 of Greaves & Nyman 1996) although their relative abundances with respect to each other are like those that we have seen.

Having measured H$^{13}$CO$^+$ in 'spiral-arm' clouds toward W49A, we can now say something conclusive about their relationship to the many features detected in higher-latitude lines of sight toward our sample of extragalactic continuum sources. The column densities of H$^{13}$CO$^+$ are $0.8\times10^{11}$ cm$^{-2}$ and $1.1\times10^{11}$ cm$^{-2}$ toward B0415+379 (Lucas & Liszt 1998), and $> 3.1\times10^{11}$ cm$^{-2}$ and $> 3.7\times10^{11}$ cm$^{-2}$ for the 'spiral-arm' clouds toward W49A, in order of increasing velocity in both cases. So the 'spiral-arm' clouds toward W49 are at least 3$-$4 times higher in column density than the thickest of the clouds we have studied previously. For the 'spiral-arm' clouds, $^{13}$CO emission is relatively strong and we conclude that they are more akin to the denser, darker, translucent objects studied by Turner (1998) (see below). Surveys of the molecular cloud ensemble in the inner Galaxy easily detect all $^{13}$CO features in emission from such common species as HCO$^+$, CS, *etc.* (Liszt 1995), which again differentiates 'spiral-arm' clouds from diffuse gas seen as discrete features at higher galactic latitude.

Given the difficulties we encountered in trying to understand the extant "spiral-arm" spectra of SiO toward W49A – the absence in our synthesis of the claimed singledish SiO feature, contamination of the higher velocity SiO absorption with the blue wing of the dimethyl ether lines, and the absence in the singledish results of the dimethyl ether emission – we hesitate to put too much stock in a detailed molecule-by-molecule comparison of abundances, for instance with the summary table of Nyman & Millar (1989). Some aspects of the comparison seem consistent with the trends we have observed and some not, but the transition from diffuse to dark material will certainly entail some changes. The high abundances of some species claimed for the 'spiral-arm' clouds may result from some degree of un-

derestimation of N($H_2$) but that for SiO toward W49A seems just to be mistaken.

We recently took spectra at the 12-m toward the off positions cited for their W49 and W51 observations by Greaves & Williams (1994), and found much prominent $^{13}$CO emission: in the $0.2 - 0.5$ K range for W49 and up to 2 K for the W51 off-source position. There was no obvious CS J=2−1 for W49. Typically, CS and other common trace species ($e.g.$ not SiO) with higher permanent dipole moments than CO appear at a level of 5−10% that of $^{13}$CO along the galactic plane (Liszt 1995). In this case, spectra toward W49A would be little affected, but the W51 continuum is somewhat weaker and off-source emission could have increased the depth of any real absorption by 0.1 in the line/continuum ratio.

### *4.2. Si and SiO in diffuse and translucent clouds*

As noted in the Introduction, the abundances we have seen are quite like those seen in emission toward translucent clouds by Turner (1998). His clouds are at least an order of magnitude denser than the diffuse clouds we have studied (the emission spectra of translucent clouds are much richer) and commensurately colder and darker. In an extensive review of quiescent, gas-phase SiO chemistry (albeit at higher density), he finds fundamental discrepancies in the rate constants available for certain important chemical reactions, which may result in changes of one order of magnitude for the SiO abundance determined by different chemical models. He finds no overall temperature dependence in the formation rate and concludes (as usual) that small SiO abundances in translucent and dark clouds must be due to a high degree of depletion of silicon from the gas phase, with $1 - \delta_{\rm Si}$ ranging from $10^{-4.3}$ in his translucent clouds to even smaller values in dark clouds.

In diffuse gas ranging up to about 1 magnitude extinction, in clouds very similar to ours, the depletion of silicon is known from optical absorption studies to be $\delta_{\rm Si} \approx 0.95$ (Savage & Sembach 1996; Tielens 1998), while in the intercloud gas $\delta_{\rm Si} \approx 0.62$. For Si, Mg, and Fe, the fraction of free material in the gas phase $1 - \delta$ varies by a similar factor 4−8 between the cloud and intercloud phases but the absolute amount of each element which remains free is quite variable with silicon being the least depleted. Differences in depletion between phases can only occur if accretion and desorption occur on shorter time scales than the material cycles between phases, implying that the loss of Si from the gas phase is an ongoing process in diffuse clouds.

Toward $\zeta$ Oph, in the gas phase, [Si]/[C] ≈ 1/80 (Savage & Sembach 1996). Along this line of sight, N(CO) $= 2.2 \times 10^{15}$ cm$^{-2}$ and N(HCO$^+$) $= 2 \times 10^{12}$ cm$^{-2}$ (Liszt & Lucas 1994): from Fig. 2, we infer N(SiO) $< 2 \times 10^{11}$ cm$^{-2}$ so that N(SiO)/N(CO) $< 10^{-4}$ and [SiO]/[Si] $< 0.01$ [CO]/[C]. This ratio is of interest because the reactions forming SiO and CO are basically the same, with Si$^+$ and C$^+$ in analogous roles. If so, something is destroying SiO 100 times faster (on a per molecule basis) than CO. Accretion onto grains occurs on a timescale comparable to the lifetime of a diffuse cloud, $10^7$ yr, not that of an individual molecule. The free-space photodissociation rates of SiO and CO are comparable and even if SiO cannot shield itself as CO does (Lee et al. 1996), the self-shielding of CO is not nearly strong enough in diffuse clouds to account for this difference. We conclude that SiO is underabundant, even compared to the known depletion level of Si.

*Acknowledgements.* The National Radio Astronomy Observatory is operated by AUI, Inc. under a cooperative agreement with the US National Science Foundation. We owe the staff at the 12-m and the Plateau de Bure our thanks for their assistance in taking the data.

The comments of the referee, Dr. E. Churchwell, are gratefully acknowledged.

We dedicate this paper to the memory of six IRAM employees, Bernard Aubeuf, Francis Gillet, Henri Gontard, David Lazaro, Roland Prayer, Patrick Vibert, who lost their lives in 1999, in two terrible accidents.

## References

Flower D.R., Pineau Des Forêts G., 1998, MNRAS 297, 1182
Greaves J.S., Nyman L.A., 1996, A&A 305, 950
Greaves J.S., Ohishi M., Nyman L.A., 1996, A&A 307, 898
Greaves, J.S., Williams P.G., 1994, A&A 290, 259
Joulain K., Falgarone E., Des Forets G.P., Flower D., 1998, A&A 340, 241
Lee H.H., Herbst E., Pineau Des Forets G., Roueff E., Le Bourlot J., 1996, A&A 311, 690
Lefloch B., Castets A., Cernicharo J., Loinard L., 1998, ApJ 504, L109
Liszt H.S., 1995, ApJ 442, 163
Liszt H.S., Lucas R., 1994, ApJ 431, L131
Liszt H.S., Lucas R., 1996, A&A 314, 917
Liszt H.S., Lucas R., 1998, A&A 339, 561
Liu S.Y., Mehringer D.M., Miao Y., Snyder L.E., 1998, ApJ 501, 680
Lucas R., Liszt H.S., 1996, A&A 307, 237, (LL96)
Lucas R., Liszt H., 1998, A&A 337, 246
Mufson S.L., Liszt H.S., 1977, ApJ 212, 664
Nyman L.A., Millar T.J., 1989, A&A 222, 231
Savage B.D., Sembach K.R., 1996, ARA&A 34, 279
Schilke P., Walmsley C.M., Pineau Des Forêts G., Flower D.R., 1997, A&A 321, 293
Tielens A.G.G.M., 1998, ApJ 499, 267
Turner B.E., 1998, ApJ 495, 804
Ziurys L.M., Friberg P., Irvine W.M., 1989, ApJ 343, 201